Optics Communications 430 (2019) 262–267

Contents lists available at ScienceDirect

Optics Communications

journal homepage: www.elsevier.com/locate/optcom

Phase compensation in digital holographic microscopy using a quantitative evaluation metric

Huaying Wang [a], Zhao Dong [a,*], Xue Wang [a], Yuli Lou [b], Sixing Xi [a]

[a] School of Mathematics and Physics, Hebei University of Engineering, No. 199, South Guangming Street, 056038, Handan, Hebei, China
[b] Faculty of Science, Kunming University of Science and Technology, No. 727, South Jingming Road, 650500, Kuming, Yunnan, China

ARTICLE INFO

Keywords:
Evaluation metric
Compensation
Phase distortion
Digital holographic microscopy

ABSTRACT

This study presents a simple metric to quantitatively evaluate the compensation of phase distortions in digital holographic microscopy. The metric calculates the difference between the minimum and maximum values in an unwrapped phase image. A phase compensation method based on the metric is proposed. Both the tilt and curvature distortions can be automatically compensated using this method, and specimen-free zones are unnecessary. It is also suitable for thick objects located in wide areas. The method using this evaluation metric has been tested and validated on several samples. With strong robustness and low computational complexity, this approach can result in accurate and effective quantitative phase imaging in holographic microscopy.

1. Introduction

Since digital holographic microscopy (DHM) provides label-free quantitative phase imaging of non-biological and biological samples with high resolution, it has been investigated continuously over the past two decades [1–7]. Gabor's original point source geometry has been used in inline DHM to obtain high-resolution images [8,9]. The reconstructed image is influenced by the twin images in this geometry [10]. It may not be suitable for larger samples. Microscope objectives have also been used to enlarge the diffracted wave in off-axis DHM. However, a curvature phase distortion will occur that can ruin the reconstructed phase images. Many physical and numerical approaches have been proposed to compensate for phase images to obtain the authentic phase of the object since the advent of microscopy [1,10–23]. For physical methods, the phase curvature can be compensated by using a twin imaging system in both arms of the DHM [11,12] or operating the microscope in telecentric architecture [13–15]. A stable and perfect matching of the optical elements is required, and in practice the phase curvature is not easy to completely eliminate [16]. In addition to physical methods, many numerical posteriori methods have been used to remove phase distortions [10,16–23]. Double exposure has been used to compensate for the phase image with high accuracy [17]. Carl et al. proposed a method based on non-diffractive reconstruction to obtain the phase image without phase distortion [10]. Both methods require recording at least two holograms with a high stable optic architecture [10,17]. Other numerical methods can complete the phase compensation using only one hologram. Ferraro et al. proposed a method for aberration compensation via lateral shear [18]. Colomb et al. proposed an automatic compensating method using a phase mask that needs a plan area (that is, the specimen-free zone) or thin specimen [19–21]. Standard polynomials [19], two-dimensional spherical functions [20], or Zernike polynomials [21] have been used to fit the mask in the reconstructed phase images. Nguyen also introduced the deep learning method to fit the mask [22], but the training process can be time-consuming. Zuo et al. proposed a numerical method based on principal component analysis with a singular value of decomposition. It also requires thin objects located in small areas [16,23]. Recently, Liu et al. proposed a method based on phase variation minimisation. A slowly varied phase profile is required for the sample in this method [24]. Min et al. presented a simple and fast phase aberration compensation method in DHM based on an analysis of the frequency spectrum of the hologram. However, it is also based on the assumption that the aberrations induced by the imaging system are much larger than the phase changes caused by the samples [25]. Although the phase images can be compensated well using the numerical methods, some remain spatially variant due to the residual error on the posteriori compensation of the quadratic phase [26]. This means that there is not a perfect compensating method to fit all situations. For the accurate use of DHM, it is best to use a metric to quantitatively evaluate the compensation. Trojans et al. proposed a thresholding and intensity summation (TIS) metric to test the correctness of the reference wave for compensating the phase [14]. This metric is calculated in two steps: (1) the wrapped phase image is

* Corresponding author.
E-mail address: handandong@163.com (Z. Dong).

https://doi.org/10.1016/j.optcom.2018.08.061
Received 22 May 2018; Received in revised form 16 August 2018; Accepted 23 August 2018
Available online 29 August 2018

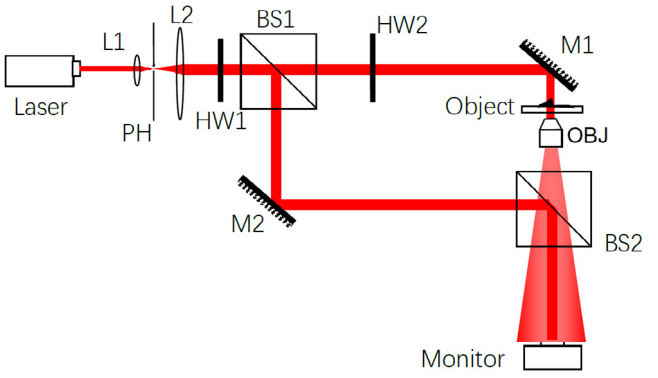

Fig. 1. The experimental setup for off-axis DHM. L: Lens, PH: pin hole, HW: half-wave plate, BS1: polarising beam splitter, BS2: non-polarising beam splitter, OBJ: objective, M: mirror.

minimised with a fixed threshold at first and (2) all of the pixels of the minimised image are added to obtain the metric value. This metric offers the possibility of quantitatively evaluating the compensated results. With the metric's help, Trujillo et al. compared the compensation quality among candidate compensating reference waves automatically [14]. The best compensated phase image was related to the highest metric value. In this paper, a simple maximum-minus-minimum (MMM) metric that calculates the difference between the minimum and maximum values in the unwrapped phase image is used to automatically compensate for the tilt as well as the curvature phase distortion introduced by the object. The quality of compensation with other methods is also evaluated with the MMM metric. The computational efficiency of the compensated methods related to the two metrics is also compared.

2. Experiment and methods

2.1. Experimental setup

The off-axis DHM for the transmission samples is used here to illustrate our method based on the MMM metric. The optic architecture is shown in Fig. 1. A laser with a wavelength (λ) of 632.8 nm is used as the light source. After being collected and expanded, the polarising beam splitter BS1 splits the beam into an object beam (O) and a reference beam (R). They interfere with each other after passing the beam splitter BS2. Two half-wave plates (HW1 and HW2) are applied to adjust the relative intensity of the two beams to make the interferogram clear. A 40× objective (OBJ) with a focus distance (f) of 0.465 mm is between the object and BS2, and the image sensor is set at the objective's image plane. If the sphere reference wave is applied to physically compensate for the curvature, an identical objective (not shown) will be used in the reference beam. Otherwise, a plane wave is used as the reference beam.

2.2. Analysis

We use the condition with the plane reference wave as an example. The hologram I can be expressed as [27]

$$I = |O|^2 + |R|^2 + OR^* + O^*R \tag{1}$$

By setting the amplitude at 1, R can be written as

$$R = \exp\left[j2\pi\left(f_x x + f_y y\right)\right] \tag{2}$$

Here, f_x and f_y are related to the spatial frequency and can be treated as the coordinates in the Fourier domain, where the origin of the coordinate system is the centre of the domain. R causes tilt distortion.

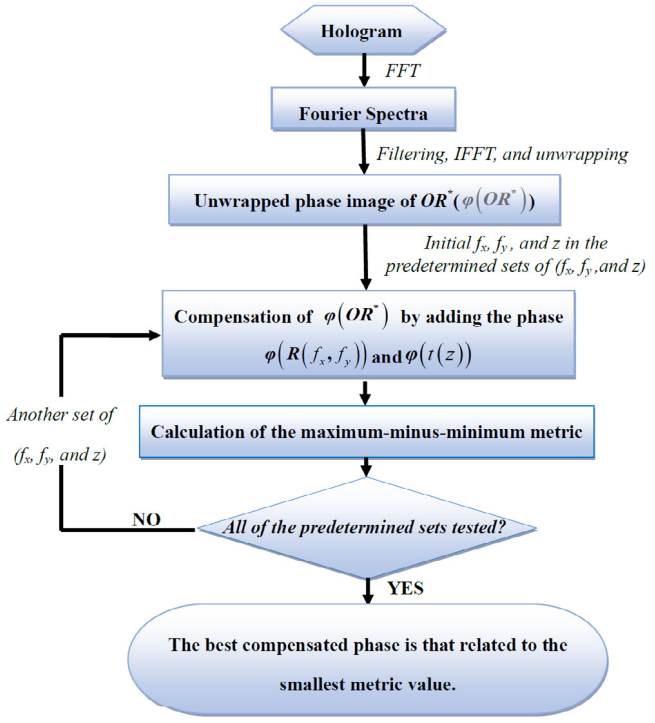

Fig. 2. Flowchart of the MMM metric compensation method.

For the object wave, as the image sensor is set at the image plane, O is expressed as [28]

$$O = \frac{1}{M} O_0\left(-\frac{x}{M}, -\frac{y}{M}\right) \exp\left[\frac{j\pi}{\lambda}\frac{x^2+y^2}{(d_i - f)}\right], \tag{3}$$

Here, d_i is the image distance. For convenience, we neglect the effect of the objective aperture and the discretisation of the image sensor. The term $\exp\left[\frac{j\pi}{\lambda}\frac{x^2+y^2}{(d_i-f)}\right]$ causes curvature distortion. As it is similar to a sphere, we call it *sphere phase distortion*. For conciseness, we set $z = d_i - f$ and $t(z) = \exp\left(-\frac{j\pi}{\lambda}\frac{x^2+y^2}{z}\right)$ and used $\varphi(\ldots)$ to express the phase of the complex amplitude in brackets. Then,

$$\varphi(t(z)) = -\frac{\pi}{\lambda}\frac{x^2+y^2}{z} \tag{4}$$

and

$$\varphi(R) = 2\pi\left(f_x x + f_y y\right) \tag{5}$$

The pairs of (f_x, f_y) in Eq. (5) were chosen using a similar method to that shown in Ref. [14]. However, when a plane reference wave is applied, rectangular patterns are in the ±1 order of the spectra [25], and the weighted centroid of the filtered zone (that is, $F\{OR^*\}$) is usually far from the point with the highest intensity. In this situation, we still set the candidate pairs (f_x, f_y) to be chosen in a circle as in Ref. [14]. Considering that the pair (f_x, f_y) related to the real compensating wave is always near the weighted centroid, it is chosen as the centre of the circle. The radius is set as the distance between the centroid and the geometrical centre of $F\{OR^*\}$. The circle is divided into rectangular grids, the sizes of which do not need to be the integer multiple of a pixel. Then the values of (f_x, f_y) are not limited to the integers. Here, the size of the grid is 0.2 pixels. The exact value of z is difficult to obtain, but the range [z_{min}, z_{max}] is easy to know in practice. In our experiment, z_{max} and z_{min} are approximately 190 mm and 200 mm, respectively, and the step of z has a value of 0.1 mm.

The flowchart for retrieving the phase distribution of O_0 is shown in Fig. 2, and the process is described as follow s: